

Relationship between GPS signals reflected from sea surfaces and surface winds: Modeling results and comparisons with aircraft measurements

Bing Lin,^{1,2} Stephen J. Katzberg,³ James L. Garrison,⁴ and Bruce A. Wielicki³

Abstract. Theoretical calculations of global positioning system (GPS) signals reflected from rough sea surfaces are discussed and compared with the aircraft measurements. The theoretical model is based on the assumption that rough sea surfaces are composed of facets, and the reflection of GPS signals from the facets can be calculated on the basis of geometric optics. In order to determine the slopes of the sea surface facets, the statistical model of *Cox and Munk* [1954] for ocean surface slopes is used. Since much of the sea surface roughness observed is at scales much less than the GPS wavelength, the dependence of the mean square slopes on frequency is taken into consideration. Model results agree well with aircraft measurements: the differences between model results and observations are within the level of experimental errors. For calm sea surfaces (near-sea-surface wind speeds $< 1 \text{ m s}^{-1}$), the correlation powers of the GPS signals are narrow functions of time delay with peak values of ~ 0 — -3 dB . In stronger wind cases (wind speeds $> 7 \text{ m s}^{-1}$), the correlation powers decrease their peak values to ~ -4 — -8 dB , significantly widen time delay responses, and shift toward the delays corresponding to path lengths longer than those of specular points. Sensitivity tests show that there is considerable potential for current or advanced GPS receiving systems to estimate near-sea-surface wind speeds: the errors in the wind speed estimates could be smaller than 2 m s^{-1} . For near-sea-surface wind directions, the maximum changes in the correlation powers of the GPS signals as a function of azimuth appear to be $\sim 0.5 \text{ dB}$ for current GPS receiving systems, which may be too small for wind direction estimation. New designs of the GPS receivers or a higher signal-to-noise ratio than that of current aircraft receivers may be needed.

1. Introduction

Ocean surface winds play important roles in the Earth's climate. They are the primary force driving ocean surface-layer circulation, enhancing the latent heat releases through sea surface evaporation, and transporting sensible heat. The ocean winds over large spatial and long time scales are usually monitored by active and passive microwave remote sensing methods, such as the SeaWinds and special sensor microwave/imager [Spencer *et al.*, 1997; Goodberlet *et al.*, 1990]. The active instruments estimate the winds by measuring the ocean surface radar backscattering cross section, while the passive ones utilize sea surface emissivity. Both the backscattering coefficient and emittance values are strongly dependent on the winds because winds are the major factor affecting sea surface roughness.

Although many studies have been made on radar backscattering during the last decades, there is very limited

knowledge, both theoretically and empirically, concerning microwave forward scattering over oceans. Recently, L band signals of the Global Positioning System (GPS) reflected from sea surfaces have been detected by airborne GPS receivers [Auber *et al.*, 1994; Garrison *et al.*, 1998]. These recorded GPS signals come from sea surface forward scattering, and it has been proposed to use these signals to monitor sea state, among other applications [Katzberg and Garrison, 1996; Katzberg *et al.*, 1998].

The concept of using GPS scattering signals for oceanography is relatively new although GPS has been used for atmospheric applications for some time [Parkinson *et al.*, 1996] (e.g., water vapor measurements [Duan *et al.*, 1996]). Using scattered signals from the existing 24 NAVSTAR satellites for ocean altimetry was first proposed by Martin-Neira [1993], and the initial aircraft experiments targeted at ocean surface forward scattering successfully detected the reflected signals by specialized time delay mapping GPS receivers [Garrison *et al.*, 1998]. The time delay mapping receivers sample the incoming signals over a range of delay times, corresponding to the different path lengths of rays reflecting off different portions of the ocean surface. Qualitatively, the measurements suggest that the stronger the winds (or the rougher the surface), the broader the time delay range of reflected signals (or the stronger the signals at longer reflection paths) [Garrison *et al.*, 1998]. Two possible approaches to analyzing the rapidly growing body of experimental data are full theoretical, based on stochastic models of rough surfaces, or phenomenological, based on

¹Center for Atmospheric Sciences, Hampton University, Hampton, Virginia.

²Also at NASA Langley Research Center, Hampton, Virginia.

³NASA Langley Research Center, Hampton, Virginia.

⁴NASA Goddard Space Flight Center, Greenbelt, Maryland.

inferred surface reflection models. Probably owing to the small amount of instrumentation that utilizes forward scattering in sea surface observations, virtually nothing exists in the literature as far as theoretical models are concerned. Theoretical analysis based on stochastic modeling has been reported by *Komjathy et al.* [1998]. In that study, the focus was primarily on the GPS signal processing, i.e., analysis of GPS satellite emitted signals, receivers' decoding (or correlation processes for the pseudo random noise (PRN) codes), and the scattering processes of ocean surfaces using a theoretical spectrum model of ocean waves. The present study differs in that the phenomenological approach mentioned above is utilized. Surface slope models built from empirical data are utilized to predict the signal recorded in the modified GPS receiver. The statistics of sea surface slopes are, in turn, determined primarily by near-sea-surface winds and the stability of the air-sea interface. This study also explores the new GPS technology for geophysical applications, in particular, wind speed and direction.

There are five sections in this paper. Section 2 briefly describes the GPS system parameters, the signal receiving characteristics, and the aircraft experiments. Section 3 discusses our model for GPS signals reflected by rough sea surfaces. Simulation results and their comparisons with observations are shown in section 4 where the frequency dependence of sea surface roughnesses is introduced and used in the GPS surface reflection model. Sensitivity of GPS reflected signals to sea surface winds is also tested in that section. It will be shown that GPS receiving systems have considerable potential for wind speed estimation. Wind direction retrievals, however, may be impractical under current system design. Finally, section 5 presents conclusions and a summary of the results of this study.

2. GPS Signals and Aircraft Experiments

The detailed GPS system design, coding/decoding, and navigation features have been discussed in many studies [e.g., *Parkinson et al.*, 1996]. Here we will outline the most important characteristics affecting the sea surface reflected signals. The GPS satellites transmit their signals at two different frequencies called L1 and L2. The carrier frequency used in this study is L1 (~1.575 GHz) and is modulated using a binary, biphasic PRN code. The signals arrive at receivers in the order of ray path lengths between GPS satellite and receiver: the shorter the path lengths, the earlier the signals reach the receivers. Since 1 bit transition in the GPS signal represents a certain minimum length of the PRN codes (referred to as a "code chip"), the GPS receivers could record output powers as a function of whole or fractional chips. For the receivers used in this study, one code chip is equivalent to ~1 ms in the temporal domain or 300 m in the spatial domain, and the data are reported every half chip of delay. In order to detect directly transferred or reflected signals from GPS satellites, cross correlation between the incoming signal and an identical replica of the PRN codes for a given satellite is performed. The output power measurements of the GPS receiver's correlators are squared values of the cross correlation of the incoming signals with the reference PRN codes. Hereafter, these power estimates are referred to as CP, for correlation power.

Assuming $A(\delta)$ is a stationary random variable that gives the relative contribution to the electric field from emitting or

reflecting points with time delays of δ , then the expected value $E\{A^2(\delta)\}$ is the signal power as a function of time delay. Thus the correlation power can be written as [*Garrison et al.*, 1998]:

$$CP(\tau) = \int_0^\infty E\{A^2(\delta)\} \Lambda^2(\tau - \delta) d\delta \quad (1)$$

where τ is the time that GPS receivers record the correlation powers and Λ function is the autocorrelation of the PRN codes and is given by

$$\Lambda(\tau) = 1 - |\tau/\tau_c|, -\tau_c < \tau < \tau_c; \Lambda = 0, \text{ otherwise} \quad (2)$$

where τ_c is the correlation time (or chip) of the receivers. Note that the term δ in (1) represents an element of time delay but that a specific time delay represents some locus on the surface through the relation of range, speed of light, and time [*Katzberg and Garrison*, 1996].

Equations (1) and (2) are the simplified formulas for GPS received powers. The Doppler effects produced by the motion of GPS transmitter and receiver on the received signal power and phase have been removed [*Parkinson et al.*, 1996; *Garrison et al.*, 1998]. The effect of Doppler shift on the signal can be ignored, since the shifts from the GPS satellites and Earth rotation are corrected by current GPS receiving systems and the speeds of aircraft carrying GPS receivers usually introduce only a insignificant additional shift. This simplification is valid in the current study, but the Doppler effects are important when spaceborne receivers are considered.

For the cases of single path length (or conventional GPS direct beam receiving cases), the power term $E\{A^2(\delta)\}$ in (1) has nonzero value at a particular time delay δ (assuming $\delta = 0$) determined by the path length between transmitter and receiver. After the convolution of (1), the outputs of the receivers at the zero time delay are equal to the signal powers and reach zero when $|\tau| > \tau_c$ because of the Λ function (equation (2)). For multiple path lengths, as is the case with ocean surface reflection, the $E\{A^2(\delta)\}$ function has nonzero values when the time delay $\delta \geq \delta_s$, where δ_s is the time delay for the shortest path length of the sea surface (or the path length from the specular point on an assumed flat sea surface). Furthermore, at any given time delay δ ($\delta \geq \delta_s$), the $E\{A^2(\delta)\}$ value is proportional to the integrated power arising from all the reflected signals with the same time delay δ . The actual digitized GPS signal power within the correlators, on the other hand, can be considered as the integral of $E\{A^2(\delta)\}$ over a short time interval.

Figure 1 is a sketch of the basic geometry of airborne GPS receiving system. The actual altitudes of GPS satellites (~26,000 km from the Earth center) are much higher than that shown in Figure 1, and the GPS ray paths are nearly parallel at the sea surface. The solid line from GPS satellite E to receiver R indicates the direct beam signals received by the aircraft. Assuming that at zero time delay the GPS signals from the satellite reach the receiver, according to (1), the correlation power only has nonzero values for the time delay τ , $-\tau_c \leq \tau \leq \tau_c$, owing to the single path length for this beam. At the center (zero time delay) of the CP function, the CP value is proportional to the signal power reaching the receiver. These direct signals are used as the reference power for this study, since the power from the GPS satellites varies with time and location. The reflected signals have multiple path lengths as indicated by the solid and dashed lines in Figure 1. It is these reflected signals that contain the information about rough sea

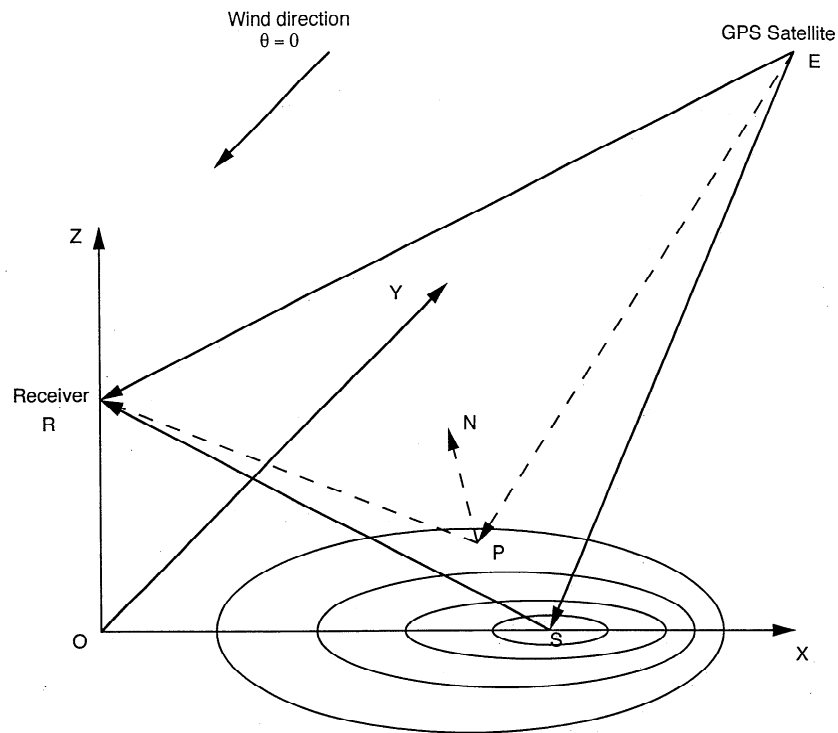


Figure 1. Sketch of the geometry of airborne Global Positioning System (GPS) receiving systems. The actual altitudes of the GPS satellites are much higher than that shown.

surfaces or near-sea-surface winds. The time delay for the shortest path length (solid bend line) is from the specular point and lags the direct path. The reflection points with equal path length form elliptical rings on the sea surfaces as shown in Figure 1 (the reasons for ellipses can be seen in section 3). The differences in the time delays between adjacent ellipses represented in Figure 1 are equal to the (generally arbitrary) signal delay steps for the GPS receiver.

The aircraft experiments (or flights) collected data on 4 different days between July and November 1997. The receiver used in this study was based on a GEC-Plessey radio frequency processing chip followed by a 12-channel correlator chip. The signal detection, control loops, data processing, and information extraction were done in a host microprocessor with a software development system that came with the receiver. Each channel could be independently controlled as to Doppler shift, satellite being detected, relative delay of the reference PRN code, and initialization. The original software was modified, so that six of the channels acted as "mother" channels in the normal tracking of the satellites, while the "daughter" channels were set to match, one for one, the satellite in its mother channel. All channels had virtually the same signal amplification. The mother channels determined the correct Doppler, approximate delay, and signal acquisition. That information was used to set the daughter channels' Doppler and starting point of the delay. The delay was then controlled in steps or swept much like an oscilloscope trace. In the software, the GPS signal was squared, averaged, and recorded, along with the georeferencing information available from the mother channels. A right-hand, circularly polarized (RHCP) and a left-hand, circularly polarized (LHCP) antenna were used to receive the direct and reflected signals,

respectively (note that the GPS satellites transmit RHCP signals, while the reflected signal is virtually always predominantly LHCP [Parkinson *et al.*, 1996]). The RHCP antenna was mounted on the top of the aircraft, and the LHCP was mounted on the lower side of the aircraft (that is, they served as up- and down-looking antennae, respectively.). Both up- and down-looking antennae had generally the same hemispheric uniform gains; thus no corrections on the gain patterns were made for this study. Owing to the multichannel feature for both up- and down-looking directions, the GPS receiving systems could track up to six GPS satellites at the same time. A total of nine cases were discussed in this study for the four experiments (for each aircraft flight, approximately two to three cases were collected). Both up- and down-looking channels were in operation during the experiments, except the first one (on July 28), in which only down-looking channels measured GPS incoming signals. The data shown later are the mean values averaged over a short period of time that have higher signal-to-noise ratio than original data. The airplane altitudes for all cases were about the same, ~ 5 km. The GPS satellite distances, elevation and azimuth angles, aircraft heights, near-sea-surface wind speeds and directions, sea and air surface temperatures, and other geophysical parameters were recorded for the experiments [Garrison *et al.*, 1998]. Table 1 is a summary of the basic parameters for these aircraft flights. It can be seen that these experiments covered wind speed from $<1 \text{ m s}^{-1}$ up to $\sim 12 \text{ m s}^{-1}$, i.e., sea state from slightly rough to rough or even very rough conditions.

3. Simulation Model

The fundamental assumption for the current calculations for the reflected GPS signals is that the ocean surface is composed

Table 1. Basic Geophysical Parameters for Aircraft Experiments

	July 28, 1997		Oct. 20, 1997		Oct. 22, 1997			Nov. 7, 1997	
	SV 30	SV 24	SV 9	SV 17	SV 5	SV 23	SV 25	SV 15	SV 29
Satellite elevation angle, deg	22.5	54.2	55.7	50.1	26.2	26.6	49.4	26.5	52.8
Aircraft altitude, km	4.5	4.5	5.4	5.4	6.8	6.8	6.8	4.9	4.9
Sea state	2	2	4—5	4—5	3	3	3	2	2
Wind speed, m s ⁻¹	< 1	< 1	12.3	12.3	8.8	8.8	8.8	7.7	7.7
Wind direction, deg	62.2	-135.5	125.4	-134.1	65.4	152	-110.9	-159.3	-88.9
Sea surface <i>T</i> , K	297.5	297.5	292.0	297.5	291.5	291.5	291.5	289.4	289.4
Surface air <i>T</i> , K	299.4	299.4	290.5	290.5	288.9	288.9	288.9	289.7	289.7

SV is satellite. Sea states of 2, 3, 4, and 5 are used to describe slight, moderate, rough, and very rough sea surface conditions, respectively. The near sea surface wind direction is the azimuth angle (or the azimuth angle difference) between the airflow and the GPS satellite.

of flat facets that act like perfectly smooth planes for electromagnetic wave (or ray) reflection. The reflectivity for perfect flat surfaces, which is dependent on incident angle of the ray and the electrical properties of the reflecting material, could be obtained from the Fresnel equations [e.g., *Beckmann and Spizzichino*, 1987]. Thus the simulation model for the GPS reflected signals is basically separated into three components. The first component is to determine the locus of all reflecting points with the same path length (or time delay), the geometry (or sea surface slope) required for the incident radiation to be reflected toward the receiver, and the reflectivity of ocean facets. The second component accounts for the probability of the ocean surface slopes as a function of near-sea-surface winds and the signal power reflected and received for each scattering point. Finally, component 3 integrates all reflected powers within the same time delay and obtains the correlation powers (receivers' outputs). Ocean surfaces usually have some areas covered by whitecaps or ocean foam, which have significantly different scattering properties from those of clear sea surfaces, and are considered in this component.

3.1. Geometry and Fresnel Reflection of GPS Signals

Although ocean surfaces are rough and their heights are varying with time owing to ocean waves, the mean surfaces could be considered as flat planes if large-scale surface slopes are zero. Because actual variations in the sea surface heights are much smaller than the path lengths of the GPS recording time steps, this plane assumption gives very small errors in the locus calculation for equal path length points over sea surfaces. Here the Earth's curvature is also neglected, which is valid for current aircraft-received GPS signals with reflection areas on the ocean surfaces generally near the specular points. The horizontal scale of the GPS signal reflection zone is usually much less than 100 km for the 32 half chips recorded by the receivers.

Assuming the sea surface is the smooth plane *xy* at height *z*=0, the receiver at point *R* (0, 0, *h*₁), and GPS satellite transmitter at position *E* (*r*₀, 0, *h*₂) illuminating the *xy* plane as indicated in Figure 1, for an arbitrary point *P* on the plane, the path length is *EP* + *PR* > *ES* + *SR*, where *S* is the specular point. The equation *EP* + *PR* = constant forms an ellipsoid in three-dimensional space with foci at *E* and *R* (if *P* is not restricted on the plane). The locus of all points on the *xy*

plane with the same path length as *P* is the cuts on the ellipsoid with the plane of *z*=0, which is an ellipse. For the GPS reflection problem studied here, the receivers record signals in constant time intervals (or half chips); thus the locus on the sea surface of the *n*th time interval can be written as

$$EP + PR = ES + SR + \Delta, z = 0 \quad (3)$$

where Δ is the distance traveled by light for *n* time intervals. Changing *n* from 0, to 1, 2, 3, etc., (3) draws a group of ellipses on the sea surface (or elliptical rings), as illustrated in Figure 1. The power recorded for each time interval is the integral within its corresponding elliptical ring of all the scattered powers in the direction of the receivers. Note that if the Earth's curvature is considered, the condition *z*=0 in (3) should be replaced by the Earth's surface equation. For example, the condition would be radius = constant for a spherical Earth assumption. Since the determination of the ellipses in (3) is straightforward, there is no need for further discussion on this issue. The detailed mathematical solution for the ellipses can be found in many studies [e.g., *Beckmann and Spizzichino*, 1987; *Katzberg and Garrison*, 1996].

Since ocean surfaces are rough and have certain slope distributions, there are finite probabilities for scattering points to have the required slopes to reflect the incident GPS signal toward a receiver (discussed in section 3.2). For an arbitrary reflecting point *P* (see, Figure 1), in order to satisfy the slope requirements, the normal vector ***n*⁰** (hereafter bold characters represent vectors, while those with superscript 0 mean unit vectors), or ***PN*** as indicated in Figure 1, of the reflection surfaces (or the facets) has to be within the plane of *EPR*, and with the angle *EPN* = angle *RPN*. Thus

$$\mathbf{n}^0 = (\mathbf{PE}^0 + \mathbf{PR}^0) / |\mathbf{PE}^0 + \mathbf{PR}^0| \quad (4)$$

The slope values in *x* and *y* directions and the incident angle θ can be easily calculated from this normal vector.

After the incident angle θ is obtained from (4), the reflectivity of ocean facets can be calculated using Fresnel equations [e.g., *Beckmann and Spizzichino*, 1987]. Let *R_v* and *R_h* be Fresnel coefficients for vertical and horizontal, linear polarization, respectively, then,

$$R_v = \frac{\epsilon \cos \theta - \sqrt{\epsilon - \sin^2 \theta}}{\epsilon \cos \theta + \sqrt{\epsilon - \sin^2 \theta}} \quad (5)$$

$$R_h = \frac{\cos \theta - \sqrt{\epsilon - \sin^2 \theta}}{\cos \theta + \sqrt{\epsilon - \sin^2 \theta}} \quad (6)$$

where ϵ is the complex dielectric constant of seawater, which is the function of sea surface temperature and salinity and the GPS wavelength [Klein and Swift, 1977]. Note that in this study, the sea surface temperature was from surface observations, while a constant value (35 practical salinity unit (psu)) is used for sea surface salinity in the model. Thus the coefficient of right- to left-hand circular polarization R_{rl} is

$$R_{rl} = (R_v - R_h)/2 \quad (7)$$

and the reflectance r for the ocean facets is $r = |R_{rl}|^2$.

3.2. GPS Reflection From Rough Sea Surface

In order to reach the GPS receiver, the incident and reflecting angles for the scattered GPS rays and the sea surface slopes in x and y directions have to meet the requirement of (4), as discussed previously. The probability of the slopes having the required angles is dependent on the rough sea surface slope distribution. Assuming the power received by the up-looking GPS antenna is I_0 , the distances between the GPS satellite and the receiver and between the satellite and surface reflection point $P(x, y, 0)$ (i.e., ER and EP in Figure 1) are D_0 and D , respectively, the reflected power dI to the direction of the receiver from the small area $d\Sigma$ containing P in the facet of rough sea surfaces would be:

$$dI(x, y) = r(I_0 D_0^2 / D^2) G(S_x, S_y) \Delta T(S_x, S_y) (d\Sigma / Ar) \quad (8)$$

where r is the right- to left-hand polarized reflectance and Ar is the area of the antenna of the GPS receiver. The term $G(S_x, S_y) \Delta T(S_x, S_y)$ is the probability of the sea surface with S_x and S_y slope values in x and y directions satisfying that the reflected rays point to the center of the down-looking antenna (in other words, S_x and S_y are the solutions of (4)). The factor $G(S_x, S_y)$ is the probability density function (PDF) of ocean surface slopes, which generally decreases with increasing angles of the slopes and is strongly related to near-sea-surface winds. The stronger the winds are, the smaller the PDF values around zero slope values and the larger the PDFs at bigger slope angles. The $\Delta T(S_x, S_y)$ factor in (8) is the small area in the slope $S_x S_y$ plane centered at (S_x, S_y) point and satisfies the requirement that the slope variations (or S_x and S_y variations in the x and y directions) within the $\Delta T(S_x, S_y)$ area of the slope $S_x S_y$ plane keep reflected rays within the direction of the down-looking antenna. It is clear that this $\Delta T(S_x, S_y)$ area (or tolerance of S_x and S_y) is decided by the size and shape of the down-looking antenna and the geometry of GPS satellite, receiver, and reflecting points. Because the gain and geometry of down-looking antenna are virtually the same as those of up-looking one for current aircraft GPS receiving systems, the ratio $\Delta T(S_x, S_y)/Ar$ is a relative value and basically not dependent on the absolute value of Ar .

The pioneering study of Cox and Munk [1954] provided detailed statistics of ocean surface slopes. On the basis of Sun glitter photographic measurements, they found that the probability density function of the ocean surface slopes (the $G(S_x, S_y)$ factor in (8)) could be expressed in a Gram-Charlier distribution, which is the product of a Gaussian distribution and a series of Hermite polynomials. The mean square slopes of the sea surfaces (or the sea surface roughnesses) in both

upwind and crosswind directions were linear functions of wind speeds, and the skewness and kurtosis (relative to the Gaussian distribution) of the PDF were weakly and statistically not significantly correlated to wind speeds, respectively. Noticeable differences in upwind and crosswind directions for the PDF represent the azimuth asymmetry of ocean surface waves in the directions. From the points of view of radiative transfer and remote sensing, the light scattering at the sea surface is generally determined by the slope PDF, which is strongly affected by wind speed and direction through the upwind and crosswind mean square slopes of rough sea surfaces.

Since the landmark Cox and Munk [1954] work, there have been continual efforts to better determine the relationships between rough sea surface slopes and near-sea-surface winds. Some of these studies agreed well with those of Cox and Munk, while others did not, even finding their mean square slopes were about a factor of 3 larger than the Cox and Munk values. Recently, Shaw and Churnside [1997] found that their and other previous measurements of sea surface slope statistics were generally consistent with those of Cox and Munk if the air-sea interface stability had been taken into account. The more stable are the air-sea interfaces, the smoother are the sea surfaces (or the smaller the mean square slopes of the sea surfaces). The mean square slope (σ^2) obtained by Shaw and Churnside is

$$\sigma^2 / \sigma_{cm}^2 = 1.42 - 2.80 Ri, -0.23 < Ri < 0.27;$$

$$\sigma^2 / \sigma_{cm}^2 = 0.65, Ri \geq 0.27 \quad (9)$$

where σ_{cm}^2 is the mean square slopes of Cox and Munk, while Ri is the reduced Richardson number with positive values (air warmer than water) meaning stable sea surfaces [Shaw and Churnside, 1997]. Note that the Cox and Munk data were measured under primarily neutral to positive stability, so the σ_{cm}^2 values would be less than those obtained under negative stability.

3.3. Received GPS Signal Power

As discussed before, the power reaching GPS receivers at the time delay τ is reflected from an ellipse with equal path length. The power $E\{A^2(\tau)\}d\tau$ received by GPS receivers in the time delay interval $d\tau$ between $\tau - d\tau/2$ and $\tau + d\tau/2$ would be the integral of all reflected powers over the elliptical ring with path length between $ES + SR + (\tau - d\tau/2)C$ and $ES + SR + (\tau + d\tau/2)C$ (compare with (3)), here C is the light speed. From (8) and assuming no whitecaps, we have

$$E\{A^2(\tau)\}d\tau = I_0 D_0^2 Ar^{-1} \int_{\tau-d\tau/2}^{\tau+d\tau/2} r D^{-2} G(S_x, S_y) \Delta T(S_x, S_y) d\Sigma \quad (10)$$

For simplicity, the boundary condition for the integral over the xy plane ($z=0$) in (10) is expressed in the form of time delay τ' due to the linear relationship between the path length and time delay, which means that during the integral, any small integrated area $d\Sigma$ must be within the elliptical ring that satisfies this condition.

The last factor needed to be considered for the received power is the effect of ocean whitecaps (or foam) on the GPS signal reflection. Both Hollinger [1971] and Wilheit [1979] found that whitecaps had some effect on the surface radiation at

microwave wavelengths. Foam regions could change the statistics of sea surface slopes, the density, and the dielectric constant of surface water, and even may violate the assumption of facets. Currently, there are almost no models to calculate the reflectance of whitecaps. Because whitecap regions generally have very weak reflection, this study assumes zero reflection over foam regions following Petty [1990]. With this simplification, the only parameter left for the radiative transfer effects of whitecaps is their area coverage.

The area coverage of whitecaps is strongly affected by near-sea-surface wind speeds. It is usually small ($< \sim 1\%$) when the speeds are less than 10 m s^{-1} , and large ($> \sim 10\%$) when the winds exceeds $\sim 20 \text{ m s}^{-1}$ [Monahan and O'Muircheartaigh, 1986; Monahan and Lu, 1990; and references therein]. This study uses the formula of Monahan and Lu [1990] to calculate the area coverage of whitecaps W and assumes that the whitecaps are randomly distributed over ocean surfaces. Because no reflection over whitecaps is assumed, the coverage of W should be considered as effective area coverage of whitecaps. Thus (10) becomes

$$E\{A^2(\tau)\}d\tau = (1-W)I_0 D_0^2 A r^{-1} \int_{\tau-d\tau/2}^{\tau+d\tau/2} G(S_x, S_y) \Delta T(S_x, S_y) d\Sigma \quad (11)$$

This equation shows that near-sea-surface winds (through the PDF function $G(S_x, S_y)$) are one of the most important factors affecting the signal power detected by GPS receivers, which potentially provide a new technique for wind remote sensing.

The correlation powers of the GPS receivers are the results of the convolution of $E\{A^2(\tau)\}$ in (11) with the A^2 function of (2), as indicated in (1). Usually, normalized values of the correlation powers, such as in the data obtained from the aircraft experiments, are calculated using the CP value in (1) divided by I_0 . Hereafter, we also call the normalized correlation power, CP. From (11) and based on the similarity between the up- and down-looking GPS receiving systems and the previous discussions, it can be assumed that this CP value is generally not a function of the particular antenna or the channel gains of up- and down-looking receiving channels. The CP value is primarily a function of the reflectivity of rough sea surfaces (or the near-sea-surface winds), the distances among GPS satellite, receiver, and ocean surfaces, and the geometry of the elliptical rings.

4. Results

To understand the aircraft measurements, this section presents results of simulations of the correlation powers using observed winds, actual satellite altitudes and elevation angles, aircraft altitudes, and other parameters. Initial simulation runs give results that are poorly consistent with aircraft measurements. Since much of the surface roughness observed is at scales much less than the GPS wavelength, frequency correction of the sea surface roughness is applied to the model. The sensitivity of the correlation power on near-sea-surface winds is also tested in this section.

4.1. Initial Simulations

To simulate the aircraft-received GPS signals reflected from rough ocean surfaces, numerical calculations of (1) and (11) are

performed. The simulated correlation powers of GPS receivers are reported at every half chip to be consistent with aircraft measurements. The model inputs are basically GPS system and geophysical parameters (i.e., frequency, polarization, time interval for half chips, GPS satellite elevation angle and altitude, aircraft altitude, near-sea-surface wind speed and direction, sea and air surface temperatures, etc.). The model coordinates are defined so that the GPS satellite is always located in the $y=0$ plane (see previous discussions and Figure 1). The wind direction defined in this study is the azimuth difference between the airflow and y axis; that is, zero azimuth angle of wind is the case when the y axis is pointing in the upwind direction of the airflow, as shown in Figure 1, and positive angles when airflows move counterclockwise.

The simulation model used here has three different versions in the statistics of sea surface roughness. The first version of the slope statistics is the original Cox and Munk [1954] model, which has full azimuth asymmetry of winds (referred to as Cox and Munk version or CM_{az} for simplicity); the second is the same Cox and Munk [1954] model with Shaw and Churnside [1997] corrections in the mean square slopes according to the air-sea interface stability, as indicated in (9) (referred to as mixed version or mix); the third is the simplified Cox and Munk [1955] model, which is a Gaussian distribution with only total slope variance for winds, i.e., isotropic (or nonazimuth asymmetry) statistics for sea surface slopes (referred to as simplified version or CM_{naz}).

The initial runs of the models were similar in result and disappointing. The simulated results using the values of the mean square slopes of ocean surfaces of Cox and Munk (or Shaw and Churnside) without GPS frequency corrections did not agree with aircraft measurements for the nine cases. The peak values are generally low, and the CP values for high time delays are large.

4.2. Frequency Correction for Sea Surface Roughness

The initial simulation runs suggested that there was at least one major deficiency within the current model causing the considerable disagreement between simulated results and aircraft measurements. Since sea surface roughness is the main factor affecting model results, the effect of the GPS wavelength on apparent slopes was the suspected cause. For example, the simulated results are too low at zero time delays and too broad at high-order times. These features are basically caused by unreasonably large sea surface roughnesses (or mean square slope values) for a particular near-sea-surface wind speed. Larger mean square slopes would produce lower probabilities of the sea surfaces with small slope angles and higher probabilities for large slope angles than those of smaller mean square slopes. Thus the simulations with the large mean square slopes lower the CP peak values and broaden the whole CP as a function of the time delay.

Since most slope values were measured at much shorter wavelengths than that of GPS used here, much of the roughness observed by those measurements is at scales very small compared with the GPS wavelength. This suggests that the ocean roughness parameter required for this simulation should be some fraction of those of Cox and Munk (or Shaw and Churnside). Theoretical studies of scattering from a Gaussian-distributed rough surface have confirmed this suspicion. It was found that radar backscattering is inversely proportional to the mean square slopes of a replica of the

surface "low-pass filtered" to the wavelength of the incident microwave radiation [Brown, 1978]. Using passive microwave measurements, Hollinger [1971] and Wilheit [1979] developed the following relationship between the mean square slopes as a function of frequency compared to those of Cox and Munk:

$$\sigma^2/\sigma_{\text{cm}}^2 = 0.3 + 0.02f \text{ } f < 35, \sigma^2/\sigma_{\text{cm}}^2 = 1 \text{ otherwise} \quad (12)$$

where f is the frequency (in GHz). It can be seen that at frequency 1.575 GHz, (12) gives only $\sim 1/3$ of the roughness of Cox and Munk. This study extends the application of the σ_{cm}^2 values in (12) not only for the mean square slopes of Cox and Munk but also for the values of Shaw and Churnside. Thus the actual sea surface roughness used in the following simulations is the value of Cox and Munk (or Shaw and Churnside) with GPS frequency reduction, that is, the frequency reduction for the mean square slopes of (12) is applied to all three versions of the model.

4.3. Simulation Results

Use of the reduced mean square slopes yielded greatly improved agreement between simulation results and observational data: the differences between the two are generally within the system errors of the current GPS receivers and experimental conditions.

Figures 2 to 5 are the simulated results for the four flights. The x axis for these figures is the time delay (in units of half chips), while the y axis is the normalized correlation power (in units of dB). The solid, dotted, and dashed curves represent the results of CM_{naz} , CM_{az} , and mix versions, respectively. Model inputs of wind speeds, azimuth angles of the winds, and satellite elevation angles are also shown in Figures 2 to 5. The aircraft measurements are plotted as well, as indicated by the pluses. The dash-dotted lines represent the noise levels of these aircraft measurements, which are between -20 and -30 dB for the cases. Each flight had two to three cases (labeled as a, b, and c in Figures 2 to 5). Except for the cases from July 28, 1997, the peak values of the GPS correlation powers recorded were basically ~ -4 to -8 dB, which was much higher than the noises of GPS receivers. The maximum CP values for the cases on July 28, 1997, would be even higher because of calmer sea surfaces (wind speeds $< 1 \text{ m s}^{-1}$; see Table 1) than other cases. Unfortunately, no normalized CP values were recorded on that day, because up-looking receivers were not available at the time of the first flight [Garrison et al., 1998]. The only recorded data were from down-looking channels on this particular day.

Theoretically, the time delays of the GPS signals detected by down-looking receivers should be later than those reflected from specular points (this study sets the recording times for the specular signals to be 0), and no correlation power could have existed at the time, one chip earlier than that of the specular reflection (see (1) and (2)). The aircraft measurements generally confirm this. One exception is the case of GPS satellite 15 on the November 7 flight (Figure 5a), in which case there are some recorded (about one chip long) CP values above noise level before the chip, -1, although the CP values were very low (~ -15 dB). The exact reasons for the short, weak signals are not known. They could be caused by various incidental error sources including the noise in the GPS receiving system or aircraft maneuver.

For the July 28, 1997, cases (Figure 2), ocean surfaces were only slightly rough, with wind speeds less than 1 m s^{-1} (Table 1). There was a large fluctuation in the speed and direction [Garrison et al., 1998]. Therefore the input value of the winds for the simulation model was chosen to be 0.5 m s^{-1} . The differences of the correlation powers for the three versions of sea roughness statistics are very small for both GPS satellites 30 (Figure 2a) and 24 (Figure 2b) cases. The simulated correlation powers are ~ -0.1 and -2.7 dB for the peak values of the two cases, respectively; and drop quickly below ~ -20 dB after one chip delay. The differences in the peak values are caused by grazing angle. There is a much larger area coverage for the first half chips in the smaller grazing angle case (Figure 2a) than in the larger angle case (Figure 2b). Thus the peak values in the GPS satellite 30 (Figure 2a) case are larger than those of satellite 24 (Figure 2b). Since the probability of large sea surface slopes is very small under calm sea surface conditions, the reflected powers in the direction of the GPS receiver away from the specular points (or in higher-order chips) would be minimum and so would be the correlation powers, which causes the width of the CP results for the two cases of Figure 2 to be narrow for all three versions of the model. The small, but noticeable differences between the results of the mix version and those of CM_{az} for the time delay greater than about one half chip for the GPS satellite 30 (Figure 2a) case are caused by the slight differences in the mean square slopes. Since there was positive air-sea interface stability on that day, there is a slightly smaller value of the mean square slopes used in the mix version. Thus the CP results for off-specular points are slightly smaller. Because the wind speeds on that day were so weak, the relative differences of the probabilities for the different versions of the slope statistics are small and the simulated CP values are similar, especially for the first couple of half chips (this feature can also be seen in Figure 2b).

The aircraft measurements on July 28, 1997, as discussed before, were recorded only by down-looking channels. Since the up-looking channels would measure a constant power (or correlation power) for each GPS satellite case (see (1) and (2)), the normalized CP values for a down-looking channel would be the CP values of the down-looking channel minus the constant in logarithm scales (or in decibels; see (1) and (11)). In order to compare simulated results with the measurements, a constant value was subtracted from the original recorded data for each case, which made the peak values plotted in Figure 2 the same as those of simulated results. Generally, the aircraft measurements agree with model simulations: the observed values had a very sharp peak, and the widths were narrow, as in the simulated results. The differences are that the measured values were slightly broader than those of simulations. Since the wind speed variations were large and the 12 hour mean speeds were much higher ($\sim 2.9 \text{ m s}^{-1}$ with 2.2 m s^{-1} standard deviation) [Garrison et al., 1998], the broadening in the measurements were not surprising. For the GPS satellite 24 (Figure 2b) case, the measured CP values in time zero and one (or in the zero and one half chips) were very close (their difference was only ~ 0.3 dB), which is significantly different from simulated results. Because the receivers used in this study reported the CP values at every half chip and had small errors in the start of the time delay mapping [Garrison et al., 1998], the errors in determining the time delay could be as much as plus or minus one quarter chip. These errors in the

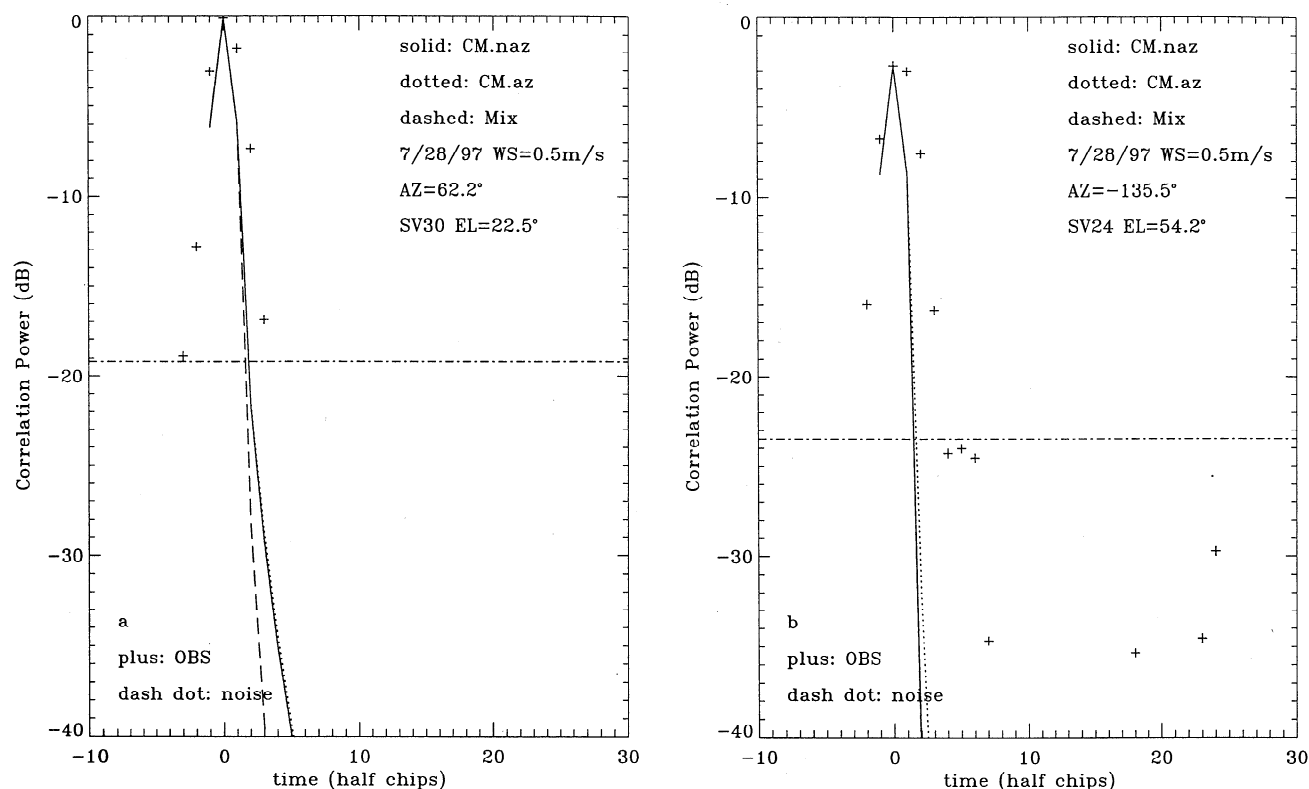


Figure 2. Simulated results of the correlation power (CP) for the July 28, 1997, GPS satellites (a) 30 and (b) 24 cases. The winds and satellite geometry are indicated.

time delay may produce the small differences in the recorded data since the observed data might miss the real peak and only had values around the zero time delay. From the data, it can be seen that small shifts in both x and y directions would improve considerably the matching between observed values and simulated results.

On October 20, 1997 (Figure 3), there were strong ($\sim 12 \text{ m s}^{-1}$), steady near-sea-surface winds. Unlike the correlation powers for the July 28, 1997, cases, the simulated results for both GPS satellites 9 (Figure 3a) and 17 (Figure 3b) cases are broad and skew toward directions (or times) later than those of specular points. The peak values for both cases are ~ -5 to -7 dB, with the slightly bigger value (~ 0.5 dB differences) for lower GPS satellite elevation angle (Figure 3b) owing to the slightly larger integral area over ocean surfaces, as discussed before. The results for different versions of the model are separated from each other, especially for those values with time delay greater than about three half chips, although they all have the same trend, with peak values at zero time and drop to -20 dB after about 10 half chips. Since this day had negative stability (see Table 1) and the mean square slopes were larger for Shaw and Churnside's [1997] rough sea slope statistics, the peak values from the mix version are about 1 dB lower than those of other two versions. For larger mean square slopes, the PDF values for larger slopes are generally bigger, thus the CP values at a higher number of half chips are greater, as shown in both Figures 3a and 3b (the mix values are larger than others at delays greater than about three half chips).

The CP differences for the simulation versions of CM_{naz} and CM_{az} are very small, especially for those of the first couple of

half chips, owing to the mean square slopes being about the same for the two versions of the model. Although the statistics of Cox and Munk [1954] have some azimuth asymmetry for sea surface slopes, the asymmetry is small, especially in the crosswind direction. Even in the upwind direction, for a moderate to strong wind of 10 m s^{-1} , the mode value of the slope statistics only shifts from 0 to $\sim -1/4$ of the mean square slopes or moves to $\sim 2^\circ$ – 3° tilt angle [Cox and Munk, 1954]. Furthermore, the GPS signal powers recorded at each half chip are the integrals of all reflecting points within an elliptical ring (see (3) and (11) and Figure 1). Since the reflection azimuth geometry (or the azimuth angle of reflection normal) related to the wind direction for different scattering points within the ring is different, the integral washes (or averages) out most of the azimuth asymmetry of the distributions of sea surface slopes. Thus the effects of wind directions on the simulated CP results are reduced (also see the sensitivity tests discussed in section 4.4). For the first couple of half chips where small sea surface slopes were needed to reflect incident GPS rays to the receiver, the effects of azimuth asymmetry on the CP values would be even weaker, because most reflected powers were decided by the main (or Gaussian) parts of the slope statistics, i.e., by the mean square slopes.

Since both up- and down-looking receivers were available during the aircraft experiment on October 20, 1997 (and later days), the normalized CP values were measured. Thus, unlike July 28 cases (Figure 2), no alignments (or tuning) between the measurements and simulations were made in the cases. Actually the alignments were not necessary for these and later

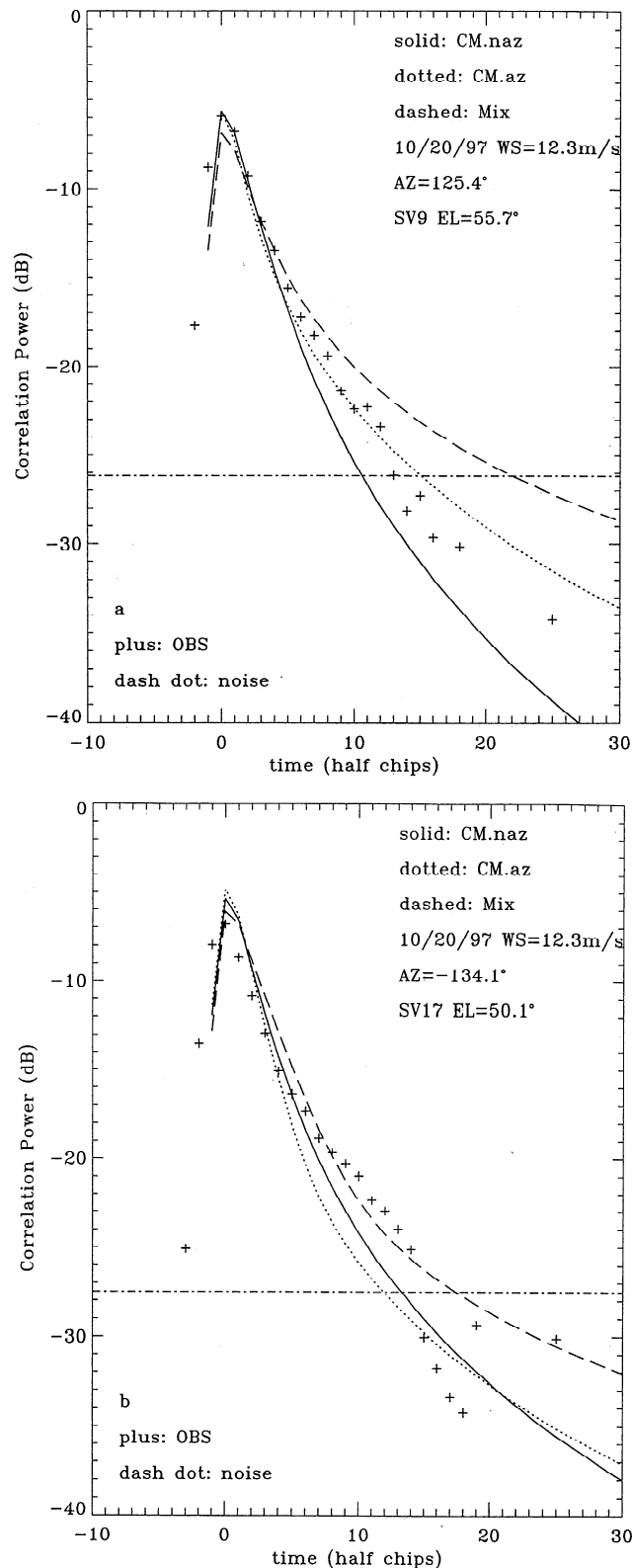


Figure 3. Same as figure 2, except for October 20, 1997, for satellites (a) 9 and (b) 17.

cases because the current GPS receiving systems have high enough accuracy to make quantitative comparisons between aircraft measurements and simulation results. Compared with aircraft measurements, the model results generally represent

well the observational data, especially for the first couple of half chips; the differences between them are much less than the system errors of current GPS receivers and experimental conditions (~ 3 dB). The broadness (or the shape) of simulated results also follow the trend of the measurements. It can be seen from Figure 3 that, unlike model simulation results, the measured peak value for the case of higher GPS satellite elevation angle (Figure 3a) was ~ 1 dB higher than that of the lower satellite elevation angle case (Figure 3b). Since the theoretically calculated differences for the two cases are only ~ 0.5 dB, and the errors in the GPS measurements are ~ 3 dB, the ~ 1 dB inconsistency between model and measurement is not significant. For the later two flights (October 22 and November 7, 1997), it is clear that the measurements support theoretical calculations (discussed next).

Figures 4 and 5 are for the flights of October 22 and November 7, 1997, respectively. On both days, there were moderate near-sea-surface winds (~ 8.8 and 7.7 m s^{-1} , respectively). Like the October 20 cases, the simulated results for the cases on the 2 days are broad and shift to longer path length directions, although the wideness and skewness are not as large as those on October 20 if the cases with similar satellite elevation angles are considered (compare Figures 4c and 5b with 3b). Comparing the results of the lower GPS satellite elevation angles with higher ones for the two days (compare Figures 4a and 4b with 4c and Figure 5a with 5b), the results with lower GPS satellite elevation angles are broader, and the peak values are higher than those of high angles, because of the reasons discussed previously. In Figure 4, the simulated results from the mix version have lower peak values, but bigger values for higher-order half chips than those of other versions because of negative air-sea interface stability of the day. For November 7, 1997, the differences between the simulated results of the mix and CM_{az} versions are small, especially for half chips less than five because of near neutral stability.

The model simulations of the CP values, like other cases, generally agree with the aircraft measurements of these 2 days. The peak values and CP variations with increasing time delays are about the same as observed values (differences are basically less than 3 dB). For the case of GPS satellite 29 on November 7, 1997 (Figure 5b), the simulated CP values at zero time delay are ~ 3.5 dB higher than those of aircraft measurements, which could be caused by gain differences of up- and down-looking receivers, instrumental noise, and small time delay mapping problems, etc., since the difference (3.5 dB) is about the magnitude of system errors of the GPS receivers. For the GPS satellite 23 cases of October 22, 1997 (Figure 4b), the measured CP values at zero and one half chip time delays were virtually the same (difference was less than 0.1 dB), which may be caused by system noise and/or the errors in time delay mapping. For these 2 days, the observed CP values were higher for the cases with lower GPS satellite elevation angles than those of higher angles, which is consistent with theoretical results.

This model study shows that the simulated results basically agree well with aircraft measurements (the differences between model and observation are usually within the errors of the GPS receivers), and the CP values recorded by the GPS receivers are strongly correlated with the mean square slopes (or roughness) of rough sea surfaces. A factor of ~ 3 reduction in the mean square slopes of ocean surfaces for L band frequencies from those of Cox and Munk or Shaw and

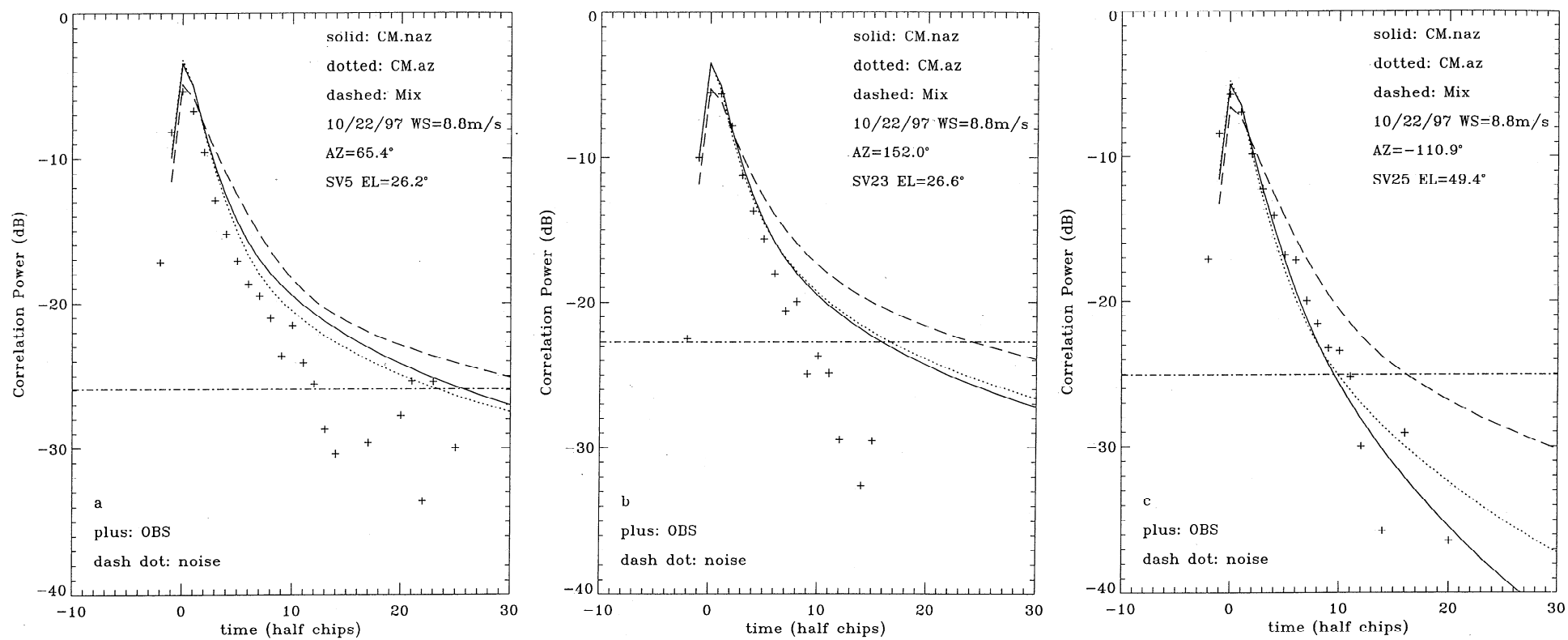


Figure 4. Same as Figure 2, except for October 22, 1997, for satellites (a) 5, (b) 23, and (c) 25.

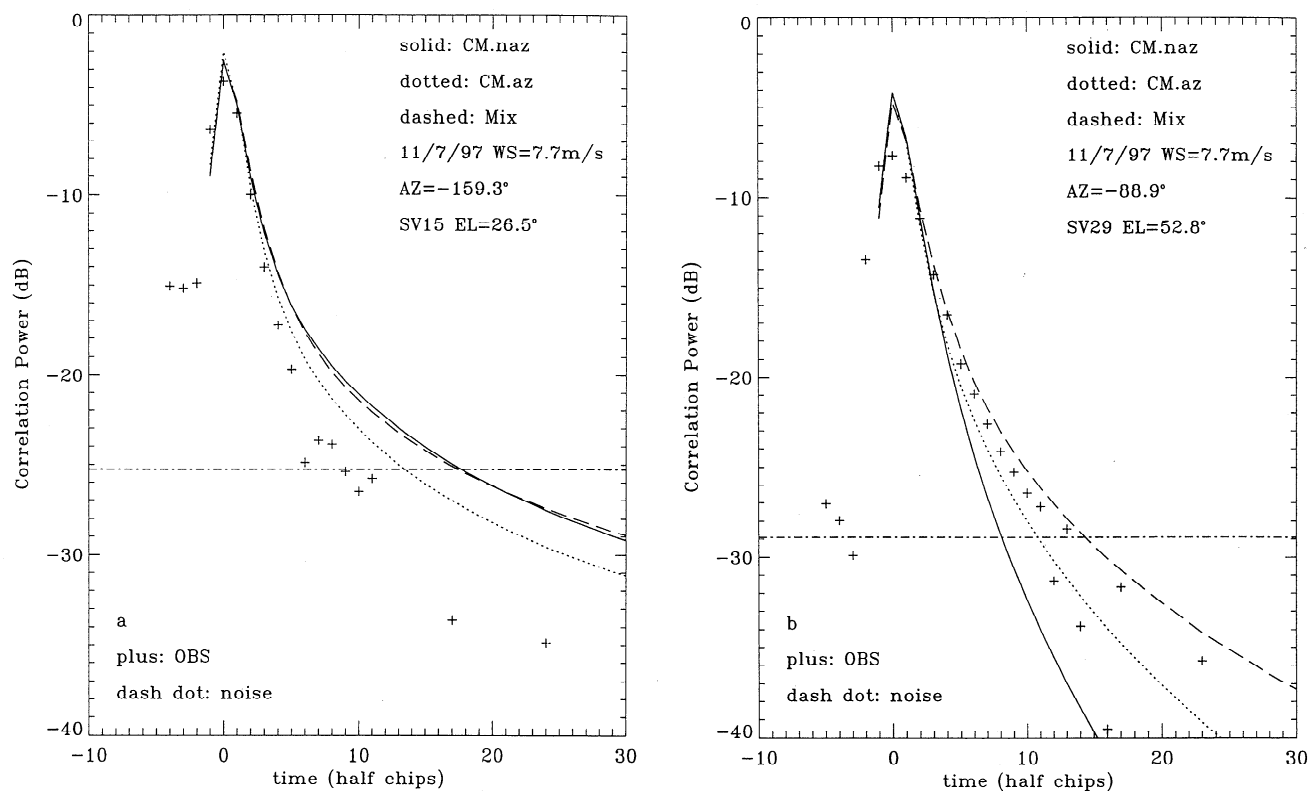


Figure 5. Same as Figure 2, except for November 7, 1997, for satellite (a) 15 and (b) 29.

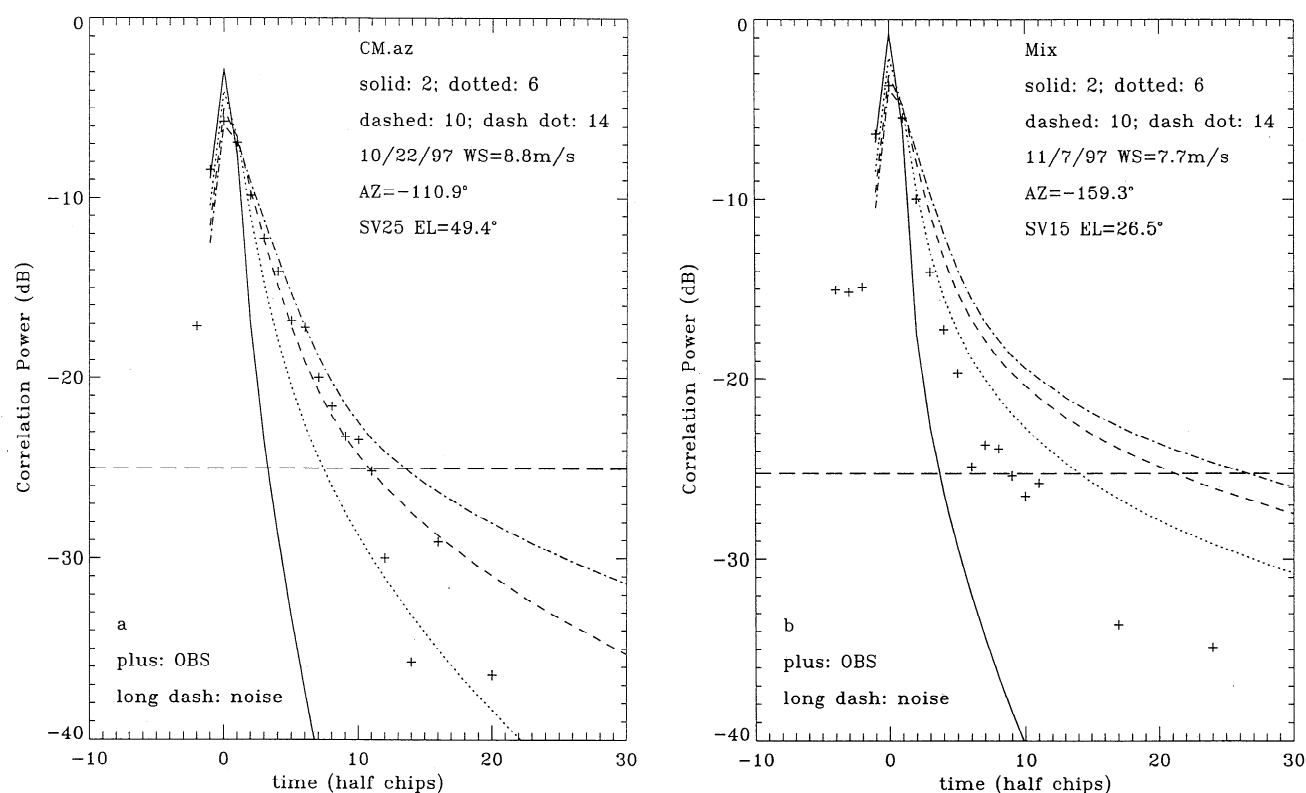


Figure 6. Same as Figure 2, except for the sensitivity tests of the CP values on the near-sea-surface wind speeds for satellites (a) 25 and (b) 15. The wind directions are the observed values. The tested speed values are 2 (solid curve), 6 (dotted curve), 10 (dashed curve), and 14 m s⁻¹ (dash-dotted curve).

Churnside may be adequate according to the comparisons between model predictions and aircraft measurements in this study and the studies of *Wilheit* [1979] and *Hollinger* [1971].

4.4. Sensitivity Tests

In order to construct the theoretical basis for the remote sensing of near-sea-surface winds using reflected GPS signals, the effects of winds (including wind speeds and directions) on the ocean surface reflection of the GPS signals were tested by changing the wind speed and direction values in the current model. The changes in the near-sea-surface winds can lead to significantly different statistics of the ocean surface slopes through the mean square slopes, the skewnesses, and the peaks of the probability density functions of the ocean surface slopes.

Sensitivity tests of CP values on near-sea-surface winds are presented for two cases (GPS satellite 25 and 15 on October 22 and November 7, respectively). The near-sea-surface winds were close to global climatological means for both cases; the GPS satellite elevation angles were about 49° and 27° , respectively; and the differences between model calculations and aircraft measurements are within the errors of the GPS receivers (see previous discussions). Since the simulated results from the version with simplified statistics of ocean surface slopes [*Cox and Munk*, 1955] are very similar to those of the other two versions, especially of the CM_{az} version (see Figures 2 — 5), and generally not dependent on near-sea-surface wind directions, only those with sea surface slope statistics containing azimuth asymmetry in wind direction (or CM_{az} and mix versions) are discussed here with each version for one case. It was found that there is almost no sensitivity difference between the tested versions.

Figure 6 shows the wind speed tests for GPS satellites 25 (Figure 6a) and 15 (Figure 6b) using the CM_{az} and mix versions, respectively, of the model. The wind speeds change from 2 m s^{-1} (solid curves), 6 m s^{-1} (dotted curves), 10 m s^{-1} (dashed curves), to 14 m s^{-1} (dash-dotted curves). The best fits of the model calculations to the aircraft observations for both cases are the simulated results with the nearest model inputs of the wind speeds to in situ measurements, i.e., the curves with 10 m s^{-1} and 6 m s^{-1} wind speeds for the two cases, respectively. Since at high time delays, CP values are generally lower than the noise levels of the GPS receiving systems, this test basically considers the GPS signals at the first seven time delay steps (time delay zero to six). Table 2 lists the sensitivity values of the CP functions for the two cases. The sensitivity of the CP peak values to the wind

speeds is basically the same for both cases ($\sim -0.23 \text{ dB m}^{-1} \text{ s}$, and $-0.22 \text{ dB m}^{-1} \text{ s}$, respectively). The CP responses in the second, half chip time delay (or the second largest CP values in time delay ≥ 0) generally do not change with wind speeds (or near zero sensitivity). The CP responses in the time delays from two to six half chips (or the next five largest CP values) increase sensitivity from ~ 0.24 (0.27) $\text{dB m}^{-1} \text{ s}$ — 0.68 (0.44) $\text{dB m}^{-1} \text{ s}$ for the model of CM_{az} (mix) version (see Table 2). For these time delays the sensitivities have different signs than those at peak CP values. The low sensitivity at a time delay of one half chip is due to the transition stage from negative to positive sensitivity.

For the near-sea-surface wind conditions similar to those tested above (or the surface wind speeds around the values tested above), the CP values at zero to six time delays could be used to estimate near-sea-surface wind speeds (as discussed above, that these CP values are considerably above noise levels even for currently used GPS receiving systems). Assuming the GPS receivers have moderate accuracy as a scatterometer, which is of the order of 1 dB or 20% relative errors [*Masuko et al.*, 1986; *Spencer et al.*, 1997] and according to the sensitivity of CP values on wind speeds discussed above (or Table 2), the errors in the estimates of near-sea-surface wind speeds would not be larger than ~ 4 — 5 m s^{-1} for each CP value at zero to six time delays (the value at time delay 1 is excluded because of its low sensitivity for winds). Thus, with six estimates of the wind speeds for each observed case, such as the cases discussed, the average errors of the estimated near-sea-surface wind speeds would be less than $\sim 2 \text{ m s}^{-1}$, which is similar to the accuracy of the special sensor microwave/imager [*Goodberlet et al.*, 1990] and Seasat scatterometer [*Nghiem et al.*, 1997]. This discussion of the errors is based upon six individual measurements in a CP function of wind speed. If function fitting between observations and model results is used in wind speed estimation, the accuracy in the estimated wind speeds would be even higher. Actually, from Figure 6, it can be seen that even for current GPS receiving systems, the best fitted results are within 2 m s^{-1} errors. Since the retrieval of wind speed (and direction) is beyond the scope of this study, detailed discussions on the wind retrievals using the reflected GPS signals will be left for future work.

The sensitivity of the CP values to wind direction appears to be very low. For 90° differences in wind direction, the absolute differences in the CP peak values are only $\sim 0.5 \text{ dB}$ and the differences for other time delays that have significant reflected GPS signals above noise levels are about of the same order, which makes the estimation on wind direction very

Table 2. Sensitivity of the Correction Power on Wind Speeds

	Time Delay (Half Chips)						
	0	1	2	3	4	5	6
CM_{az} , SV 25, Oct. 22, 1997	-0.23	-3.5×10^{-2}	0.24	0.44	0.57	0.64	0.68
mix, SV 15, Nov. 7, 1997	-0.22	5.1×10^{-4}	0.27	0.40	0.44	0.43	0.41

The units for these sensitivity values are $\text{dB m}^{-1} \text{ s}$. CM_{az} refers to the *Cox and Munk* [1954] model case with full azimuth asymmetry of winds. mix is the same model with *Shaw and Churnside* [1997] corrections. See text for details.

difficult. Figure 7 plots the results of the sensitivity tests as in Figure 6, except for wind direction. In the simulation, in situ measured wind speeds are used as the inputs, while the wind directions are set to be 0° (solid curves), 30° (dotted curves), 60° (dashed curves), and 90° (dash-dotted curves). Table 3 provides the corresponding sensitivity values for the two cases. Figure 7 and Table 3 express, at least in the sense of model simulations, that the reflected GPS signals obtained by current receiving systems have limited information about wind direction. For example, the changes in the CP values at time zero for 90° shifts of wind directions are only ~ -0.34 and -0.53 dB for the two cases, respectively, and at other times, the variations of CP values are also very small (see Table 3). The main reason for the low sensitivity is that the GPS signal powers reaching the receivers are the integral of all reflections from an elliptical ring which washes out the unique information of the azimuth dependence of sea surface slopes at each reflecting facet (see equation (11) and Figure 1). For the cases discussed here, the viewing azimuth angles change from $\sim 10^\circ$ to as large as more than 30° for the zero to six time delays. Moreover, during the integration over an elliptical ring, the places with smaller sea surface slope angles (or with viewing angles closer to those of specular points) are much more heavily weighted in the received GPS powers than those regions with larger angles. For these small slope areas, the changes of the slope probability with different azimuth angles are minimal owing to the Gaussian-like function of the slope PDF. This feature can be seen clearly in Table 3 for the high time delays, where the viewing angle deviation of received GPS rays from those of specular points are larger for the outer rings, so are the changes of the PDF with the azimuth angles.

Thus the sensitivity increases with the time delays. Besides forward versus backward rough sea surface scattering, the integration over elliptical rings is one of the major differences between the current GPS technique and conventional scatterometry. In order to avoid the integration, directional GPS receiving antennae might be considered.

5. Discussion and Summary

Three versions of the current simulation model have been evaluated to assess their ability to describe the GPS reflected signal. Although the results from the CM_{naz} version are generally as good as those of the other two versions (see Figures 2 to 5), the version cannot simulate the azimuth dependence of the rough sea surface slopes driven by the near-sea-surface wind speeds and directions. This version of the model may not be useful for future studies of the near-sea-surface winds for the GPS receiving systems designed to remotely sense not only speed but also direction. The CM_{az} version of the model has generally smaller mean square slopes than the mix version for near neutral and negative stability conditions (see (9)), and thus narrower CP responses. Since there are only limited observed cases in this study and the errors in the CP measurements (~ 3 dB) are usually larger than the differences between the simulated results of the two versions of the model, it is very hard to judge which version is better. More experiments are needed.

In the theoretical part of the study (see (8) and other related equations), a constant gain for all up- and down-looking channels at any zenith and azimuth angles is assumed [Garrison et al., 1998]. Thus no gain factors are shown in the

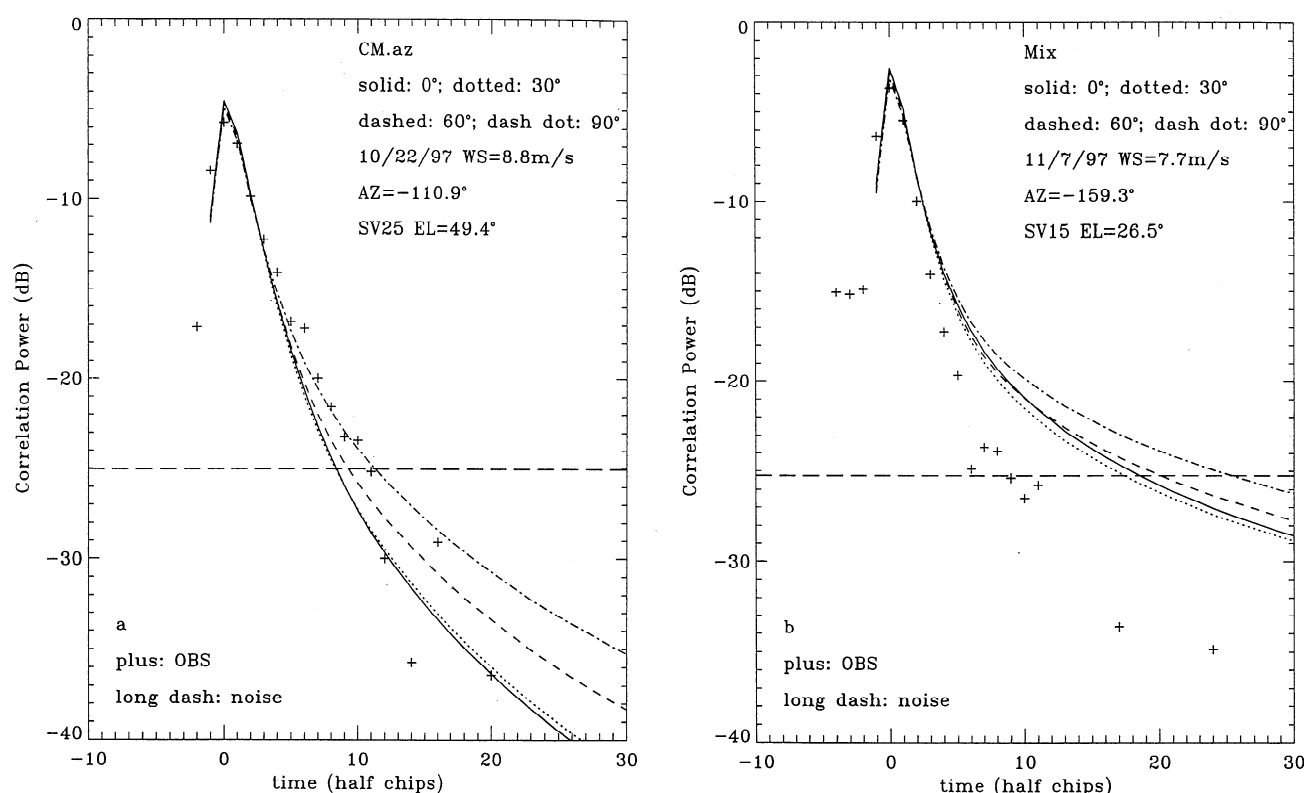


Figure 7. Same as Figure 6, except for the sensitivity tests of the CP values on the near-sea-surface wind directions. The wind speeds are the observed values. The tested direction values are 0° (solid curve), 30° (dotted curve), 60° (dashed curve), and 90° (dash-dotted curve).

Table 3. Sensitivity of the Correction Power on Wind Directions

	Time Delay (Half Chips)						
	0	1	2	3	4	5	6
CM _{az} , SV 25, Oct. 22, 1997	-0.36	-0.42	-0.28	8.4×10^{-2}	0.54	1.0	1.6
mix, SV 15, Nov. 7, 1997	-0.53	-0.44	-5.0×10^{-2}	0.27	0.35	0.38	0.47

The units for these sensitivity values are dB 90° ⁻¹.

theoretical equations. According to the sensitivity tests of CP function on near-sea-surface winds, the errors in the GPS receivers should be controlled within ~ 1 dB (or $\sim 20\%$ relative error) to keep the estimated near-sea-surface wind speed values within 2 m s^{-1} . The 1 dB errors may be lower than the errors of the GPS receivers currently used. Better calibration of the gains for both zenith and azimuth angles are needed in the application of GPS receiving systems to ocean measurements. Since both up- and down-looking channels are used simultaneously, the calibration could be done over ground, letting the two receivers look at the same GPS satellites, rotating the antenna viewing angles and switching signal processing channels. This kind of test on the gains of the antennae would provide better quantification of the gains, instead of assuming a constant for all channels as was done in this study. Another issue related to the errors in CP functions is the accuracy of time delay mapping of the GPS receivers. The shifts in time delays would cause a few decibel error in the recorded CP signals, especially for peak values, as discussed in previous sections. Better calibration in the GPS receivers for near-sea-surface wind estimation, as seen in section 4.3, will significantly improve the model studies and, furthermore, may enhance other applications in oceanic and atmospheric sciences.

The sensitivity tests of the GPS reflected CP signals on near-sea-surface wind directions show that the CP values have only very weak changes with changes in wind directions for the systems used here owing to the integration over elliptical rings. In order to remotely sense wind directions, the system designs may need some change unless the signal-to-noise ratio for current receiving systems can be increased significantly. High gain, directional antennae are one choice, which would be similar to scatterometer cases, except the GPS systems receive forward scattering signals while scatterometers obtain backward reflection. Because of the azimuth dependence of the roughnesses of ocean surfaces due to wind speeds and directions, at least three independent GPS observations may be needed for single ocean spot over short periods if the characteristics of forward scattering are similar to those of backward scattering. The advantage of this concept is that both wind speeds and directions could be estimated from the multiple measurements of the reflected GPS signals. The disadvantage is that observational coverage for certain periods of time is reduced due to the multiobservation requirements. This multiobservation issue should be investigated before future aircraft or satellite GPS reflection experiments use high-gain directional antennae for this specific application.

Another choice to avoid the "washout" in the integration over elliptical rings is to use Doppler filtering. This method can separate the currently integrated rings into certain Doppler bands, reduce the mixture in wind directions in the reflected GPS signals recorded by the receivers, and may even avoid the minimal azimuth sensitivity regions within an elliptical ring. Since the CP signals obtained by this method may still come from two or more different reflecting areas (or may still be the combinations of the reflected powers of two or more different wind directions related to the reflection normals of scattering points), the sensitivity of the CP functions on wind directions (and speeds) needs to be tested theoretically and experimentally. Furthermore, the signal-to-noise ratio for this kind of Doppler filtering system would need to be higher than those of currently used systems because the reflected GPS signals would be much weaker under the influence of a continuum of Doppler shifts.

This study has addressed a new technique, GPS sea surface forward scattering, theoretically and compared the model results with aircraft measurements. Generally, the simulation results agree well with observations. This study has shown that sea surface roughness models can adequately describe characteristics of measured GPS reflected signals. Since near-sea-surface winds are one of the key parameters affecting the mean square slopes of sea surfaces, the current GPS receiving systems or some improved designs may be used for the remote sensing for near-sea-surface winds. The errors in the wind speed estimates can be lower than $\sim 2 \text{ m s}^{-1}$ for current receivers, if they are well calibrated and utilize the maximum available signal to noise. Wind direction appears to be difficult to estimate using current receiver designs for sea surface reflected GPS signals. Some designs, such as those with high gain directional antennae, may overcome this shortcoming. Even at the present stage, both theoretical and experimental studies show that the new forward scattering microwave technology discussed in this study has considerable potential for applications in the oceanic and atmospheric sciences.

Acknowledgments. The authors thank Bill Smith and Gary Gibson for their support and suggestions on this study. This research is part of the Clouds and the Earth's Radiant Energy System under the NASA Earth Observing System. One of the authors (B.L.) gratefully acknowledges support from NASA under grant NAG-1-1963.

References

- Auber, J.-C., A. Bibault, and J.-M. Rigal, Characterization of multipath on land and sea at GPS frequencies, paper presented 7th

- International Technology Meeting of the Satellite Division of the Institute of Navigation, Salt Lake City, Utah, Sept. 23, 1994.
- Beckmann, P., and A. Spizzichino, *The Scattering of Electromagnetic Waves From Rough Surfaces*, Artech House, Norwood, Mass, 1987.
- Brown, G.S., Backscattering from a Gaussian distributed perfectly conducting rough surface, *IEEE Trans. Antennae Propag.*, AP-26, 472-482, 1978.
- Cox, C.S., and W. Munk, Statistics of the sea surface derived from sun glitter, *J. Mar. Res.*, 13, 198-225, 1954.
- Cox, C.S., and W. Munk, Some problems in optical oceanography, *J. Mar. Res.*, 14, 63-78, 1955.
- Duan, J., et al, GPS meteorology: Direct estimation of the absolute value of precipitable water, *J. Appl. Meteorol.*, 35, 830-838, 1996.
- Garrison, J.L., S.J. Katzberg, and M.I. Hill, Effect of sea roughness on bistatically scattered range coded signals from the Global Positioning System, *Geophys. Res. Lett.*, 25, 2257-2260, 1998.
- Goodberlet, M.A., C.T. Swift, and J.C. Wilkerson, Ocean surface wind speed measurements of Special Sensor Microwave/Imager (SSM/I), *IEEE Trans. Geosci. Electron.*, GE-28, 832-828, 1990.
- Hollinger, J.P., Passive microwave measurements of sea surface roughness, *IEEE Trans. Geosci. Electron.*, GE-9, 165-169, 1971.
- Katzberg, S.J., and J.L. Garrison, Utilizing GPS to determine ionospheric delay over the ocean, *NASA Tech. Memo.*, TM-4750, 1996.
- Katzberg, S.J., N.S. Coffee, J.L. Garrison, and H.R. Kowitz, Method and system for monitoring sea state using GPS, patent application, U.S. Patent and Trademark Office, Arlington, Va., 1998.
- Klein, L.A., and C.T. Swift, An improved model of the dielectric constant of sea water at microwave frequencies, *IEEE J. Oceanic Eng.*, OE-2, 104-111, 1977.
- Komjathy, A., V. Zavorotny, P. Axelrad, G. Born, and J. Garrison, GPS signal scattering from sea surface: Comparison between experimental data and theoretical model, paper presented at Fifth International Conference on Remote Sensing for Marine and Coastal Environments, Environ. Res. Ins. of Mich. International, San Diego, Calif., October 5-7, 1998.
- Martin-Neira, M., A passive reflectometry and interferometry system (PARIS): application to ocean altimetry, *ESA J.*, 17, 331-355, 1993.
- Masuko, H., K. Okamoto, M. Shimada, and S. Niwa, Measurement of microwave backscattering signatures of ocean surface using X band and Ku band airborne scatterometers, *J. Geophys. Res.*, 91, 13,065-13,083, 1986.
- Monahan, E.C., and I.G. O'Muircheartaigh, Whitecaps and the passive remote sensing of the ocean surface, *Int. J. Remote Sens.*, 7, 627-642, 1986.
- Monahan, E.C., and M. Lu, Acoustically relevant bubble assemblages and their dependence on meteorological parameters, *IEEE J. Oceanic Eng.*, 15, 340-349, 1990.
- Nghiem, S.V., F. Li, and G. Neumann, The dependence of ocean backscatter at Ku Band on oceanic and atmospheric parameters, *IEEE Trans. Geosci. Remote Sens.*, GE-35, 581-600, 1997.
- Parkinson, B.W., J.J. Spilker, P. Axelrad, and P. Enge, Global positioning system: Theory and applications, vols. 1 and 2, Am. Ins. of Aeronaut. and Astronaut., Washington, D. C., 1996.
- Petty, G. W., On the response of the special sensor microwave/imager to the marine environment—Implications for atmospheric parameter retrievals, Ph.D. dissertation, Dep. of Atmos. Sci., Univ. of Wash., Seattle, 1990.
- Shaw, J.A., and J.H. Churnside, Scanning-laser glint measurements of sea-surface slope statistics, *Appl. Opt.*, 36, 4202-4213, 1997.
- Spencer, M.W., C. Wu, and D. Long, Tradeoffs in the design of a spaceborne scanning pencil beam scatterometer: application to SeaWinds, *IEEE Trans. Geosci. Remote Sens.*, GE-35, 115-126, 1997.
- Wilheit, T.T., A model for the microwave emissivity of the ocean's surface as a function of wind speed, *IEEE Trans. Geosci. Electron.*, GE-17, 244-249, 1979.

J.L. Garrison, NASA Goddard Space Flight Center, Mail Code 572, Greenbelt, MD 20771.

S.J. Katzberg, B. Lin (corresponding author), and B.A. Wielicki, NASA Langley Research Center, MS 420, Hampton, VA 23681-2199 (bing@front.larc.nasa.gov)

(Received October 26, 1998; revised April 2, 1999; accepted June 3, 1999.)